High-temperature ion-thermal behavior from average-atom calculations

Damian C. Swift,[1,*] Mandy Bethkenhagen,[1,†] Alfredo A. Correa,[1] Thomas Lockard,[1] Sebastien Hamel,[1] Lorin X. Benedict,[1] Philip A. Sterne,[1] and Bard I. Bennett[2]

[1]*Lawrence Livermore National Laboratory, 7000 East Avenue, Livermore, California 94551, USA*

[2]*Los Alamos National Laboratory, P.O. Box 1663, Los Alamos, New Mexico 87545, USA*

(Received 21 May 2019; revised manuscript received 31 December 2019; accepted 6 March 2020; published 4 May 2020)

Atom-in-jellium calculations of the Einstein frequency were used to calculate the mean displacement of an ion over a wide range of compression and temperature. Expressed as a fraction of the Wigner-Seitz radius, the displacement is a measure of the asymptotic freedom of the ion at high temperature, and thus of the change in heat capacity from six to three quadratic degrees of freedom per atom. A functional form for free energy was proposed based on the Maxwell-Boltzmann distribution as a correction to the Debye free energy, with a single free parameter representing the effective density of potential modes to be saturated. This parameter was investigated using molecular dynamics simulations, and found to be ~0.2 per atom. In this way, the ion-thermal contribution can be calculated for a wide-range equation of state (EOS) without requiring a large number of molecular dynamics simulations. Example calculations were performed for carbon, including the sensitivity of key EOS loci to ionic freedom.

DOI: 10.1103/PhysRevE.101.053201

I. INTRODUCTION

Accurate equations of state (EOS) are essential to understand stellar and planetary formation and evolution, astrophysical impacts, and engineering challenges such as the development of thermonuclear energy sources. However, the behavior of the ionic heat capacity of condensed matter at temperatures between melting and the formation of an ideal plasma is poorly understood, limiting the insight and accuracy of theoretical EOS. Wide-ranging EOS [1] are almost invariably constructed using empirical models originally derived as approximate representations of observations of the variation of the heat capacity in the liquid of metals of low melting point at one atmosphere [2], and assumed to apply at arbitrary compression [3,4]. Experiments to test or improve on this assumption are challenging: where even attempted, uncertainties on measurements of the temperature of warm dense matter are typically greater than 10% (see, for instance, [5,6]), which is not adequate to distinguish the details of the ion-thermal heat capacity.

The most rigorous theoretical techniques applicable are path integral Monte Carlo (PIMC) and quantum molecular dynamics (QMD), in which the kinetic motion of an ensemble of atoms is simulated, where the distribution of the electrons is found with respect to the changing location of the ions using quantum mechanics [7,8]. The energy of the ensemble is determined from an average over a sufficient time interval, and the heat capacity can be found from the variation of energy with temperature. This procedure is computationally expensive, requiring $o(10^{16})$ or more floating-point operations per state to determine the ionic heat capacity using QMD, equivalent to thousands of CPU hours per state; PIMC requires roughly an order of magnitude more. It is typically deemed impractical to perform these simulations for matter around or below ambient density and above a few tens of electron volts using QMD, limiting the regions of state space over which the EOS models can be calibrated in this way.

Recent PIMC and QMD results have indicated that the simpler approach of calculating the electron states for a single atom in a spherical cavity within a uniform charge density "jellium" of ions and electrons, representing the surrounding atoms, reproduces the electronic component of their more rigorous EOS models [9,10]. This atom-in-jellium approach has been used previously to predict the electron-thermal energy of matter at high temperatures and compressions [11], as an advance over Thomas-Fermi and related approaches [12]. A development of atom-in-jellium was used to estimate ion-thermal properties using the Debye model [13], and we have found that it can be used to construct the complete EOS [14]. However, the model as originally implemented did not account for the decrease in ionic heat capacity at high temperatures as the ions cease to be caged between their neighbors, losing the contribution from potential energy. We also noted cases where the atom-in-jellium Debye model deviated from more rigorous calculations.

In the work reported here, we extend the atom-in-jellium ion-thermal model developed previously [14] to estimate the asymptotic freedom of ions at high temperature, and hence predict the form of the heat capacity of matter in the fluid-plasma regime. Because of the efficiency of average-atom calculations, this approach should enable EOS models to be constructed with consistently accurate electronic contributions and the correct ion-thermal behavior over a wide range of

*dswift@llnl.gov

†Present address: Ecole Normale Supérieur de Lyon, 15 parvis René Descartes, 69342 Lyon, France.

states from expanded to compressed matter and over the full range of temperatures relevant to stellar and planetary interiors, and thermonuclear fusion science.

We consider carbon (C) as an interesting test case because it is notable for exhibiting directional bonds that also change in strength and nature under compression, leading to multiple solid phases on compression. The atom-in-jellium method does not distinguish between different structural phases, and so is inherently unable to capture the details of and changes in bonding. C is thus a particularly challenging material to treat with the atom-in-jellium model. The relative contribution to the EOS of the high-temperature decrease in the ionic heat capacity falls with atomic number Z: for high Z, the electron-thermal contribution to the heat capacity becomes dominant in the fluid-plasma regime because of the greater number of electrons. The accuracy of a good EOS model and good state measurements at high pressure and temperature is typically $o(1\%)$, so it is most practical to focus on elements where the effect on the EOS is at the level of at least several percent, i.e., $Z \lesssim 10$; this range does cover the vast majority of matter in the universe. Of these elements, C is particularly convenient for experiments, being readily available and presenting relatively little complication in the preparation of samples, being nontoxic, chemically stable, and solid at ambient conditions. Because of its importance for inertial confinement fusion studies, C has been the subject of extensive previous studies, including the construction of a state-of-the-art multiphase EOS model [9].

II. PREVIOUS ION-THERMAL MODELS

As condensed matter is heated from absolute zero, the heat capacity of the ions rises from zero as vibrational modes are excited. If all modes are excited before any dissociation occurs, the ionic heat capacity for quadratic degrees of freedom reaches $3k_\mathrm{B}$ per atom, where k_B is the Boltzmann constant, representing three kinetic and three potential modes [15]. The attractive potential between atoms has a finite depth, and once an ion has more energy, it behaves as a free particle with only kinetic modes available to it, and thus contributes $3k_\mathrm{B}/2$ to the heat capacity.

The instantaneous separation and velocity of the ions are described by a distribution, and the most appropriate description of the ion energies is also by a distribution. Even at low temperatures some ions are free, and even at high temperatures some ions are bound. The detailed distribution of ion energies depends on the shape of the interatomic potential as well as the temperature, which complicates the analysis.

EOS models have been constructed using very simple estimates of the ion-thermal contribution, such as a constant specific heat capacity which may be the value at STP, $3k_\mathrm{B}$ per atom, or $3k_\mathrm{B}/2$ per atom [16]. A generalization has been to use the Debye model [17], which assumes a simple form for the phonon density of states (PDOS), proportional to $\hbar\omega^2$ for phonon frequencies $0 \leqslant \omega \leqslant k_\mathrm{B}\theta_\mathrm{D}$, and 0 for higher ω. This model captures the rise of ion-thermal heat capacity from zero to $3k_\mathrm{B}$ per atom as modes are excited, but does not capture the detailed heat capacity arising from the actual PDOS. EOS models can be constructed using more accurate PDOS [18], though, in practice, because integrations are performed over the PDOS, the EOS is not sensitive to the full detail of the spectrum, and high-fidelity models have been constructed using a combination of a few Debye frequencies instead [19]. More importantly for the present study, the Debye model ignores the asymptotic freedom of the ions at high temperature.

In the ion-thermal model developed for use with atom-in-jellium calculations [13], perturbation theory was used to calculate the Hellmann-Feynman force on the ion when displaced from the center of the cavity in the jellium. Given the force constant $k = -\partial f/\partial r$, the Einstein vibration frequency $\nu_e = \sqrt{k/m_a}$ was determined, where m_a is the atomic mass, and hence the Einstein temperature $\theta_\mathrm{E} = h\nu_e/k_\mathrm{B}$. The Debye temperature θ_D was inferred from θ_E, by equating either the ion-thermal energy e_i or the mean-square displacement $\bar{u^2}$, giving slightly different results. These calculations are, respectively,

$$e_i \frac{m_a}{3k_\mathrm{B}T} = x_\mathrm{E}\left[\frac{1}{\exp(x_\mathrm{E})+1} + \frac{1}{2}\right] = D_3(x_\mathrm{D}) + \frac{3}{8}x_\mathrm{D} \quad (1)$$

and

$$\bar{u^2}\frac{m_a}{3\hbar^2} = \frac{1}{\theta_\mathrm{E}}\left[\frac{1}{\exp(x_\mathrm{E})-1} + \frac{1}{2}\right] = \frac{1}{\theta_\mathrm{D}}\left[\frac{D_1(x_\mathrm{D})}{x_\mathrm{D}} + \frac{1}{4}\right], \quad (2)$$

where $x_\mathrm{E} = \theta_\mathrm{E}/T$, $x_\mathrm{D} = \theta_\mathrm{D}/T$, and D_i is the Debye integral

$$D_i(x) \equiv \frac{i}{x^i}\int_0^x \frac{x^i\,dx}{e^x - 1}. \quad (3)$$

The ion-thermal free energy was then calculated from

$$f_i = k_\mathrm{B}T\left[3\ln(1 - e^{-\theta_\mathrm{D}/T}) + \frac{9\theta_\mathrm{D}}{8T} - D_3(\theta_\mathrm{D}/T)\right], \quad (4)$$

where $\frac{9}{8}k_\mathrm{B}\theta_\mathrm{D}$ is the zero-point energy. Unusually, θ_D is a function of temperature as well as compression, effectively because changes in ionization can result in a change to the stiffness and hence the vibration frequency. However, despite the accuracy of atom-in-jellium predictions of the electronic EOS [14], and the ingenuity of using perturbations of the ion from equilibrium to predict θ_D and hence f_i for condensed matter, the lack of a treatment of the high-temperature ionic heat capacity is a notable limitation in an approach otherwise suited to warm dense matter.

An approach used widely in constructing EOS for fluid-plasma applications is the Cowan model [3], in which the heat capacity is assumed to vary as

$$c_v = \frac{3}{2}k_\mathrm{B}\left\{1 + \min\left[1, \left(\frac{T}{T_m(\rho)}\right)^{-1/3}\right]\right\}, \quad (5)$$

where $T_m(\rho)$ is the melting temperature as a function of mass density ρ. The effect of the term in brackets is for the potential modes to fall as $(T/T_m)^{-1/3}$ for $T > T_m$, and for c_v to be held at $3k_\mathrm{B}$ for $T \leqslant T_m$. Variants of the Cowan model have been used with more general dependence on T/T_m, also treating the latent heat of melting in *ad hoc* fashion as an increased ionic heat capacity over a finite temperature range [4].

QMD studies of carbon [9] found that the heat capacity dropped more abruptly than in the Cowan model, and were

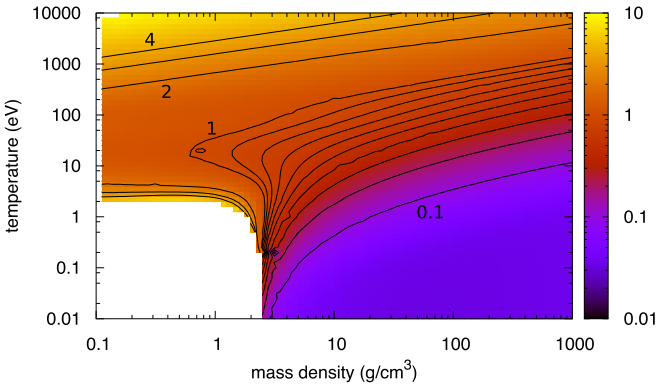

FIG. 1. Root-mean-square fractional displacement $u_{\rm rms}/r_{\rm WS}$ calculated for carbon using atom-in-jellium theory. Contours shown are from 0.1 to 1.0 at intervals of 0.1, and then 2.0 to 4.0 at intervals of 1.0. A fractional displacement of 1 would correspond to ionic freedom, ignoring the velocity distribution of the ions.

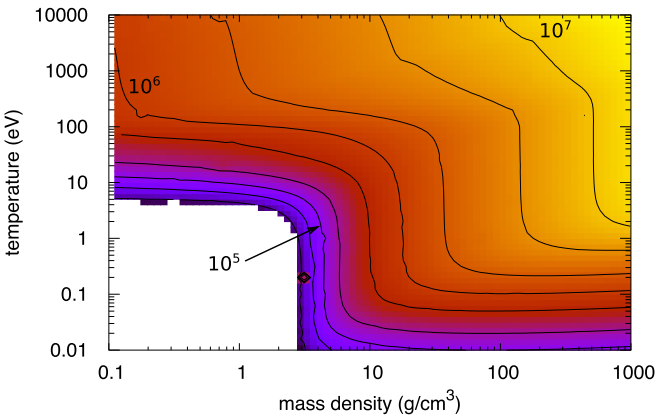

FIG. 2. Characteristic binding temperature $T_b = Tr_{\rm WS}^2/\bar{u^2}$ calculated for carbon. Contours shown are $\{1, 2, 5\} \times 10^{\{4,5,6,7\}}$ K. Where contours of T_b are not vertical, its temperature dependence is significant.

represented better as a free energy of the form

$$f_i = f_b - k_{\rm B}T \ \ln\left[\mathrm{erf}\left(\sqrt{\frac{T_r}{T}}\right) - \sqrt{\frac{4T_r}{\pi T}}e^{-T_r/T}\right], \qquad (6)$$

where f_b is the free energy of bound ions and $T_r(\rho)$ is a reference temperature curve determined from QMD. This approach appears to be as accurate as QMD can achieve, but is limited by the restricted range of states accessible in practice to QMD.

III. ASYMPTOTIC FREEDOM OF IONS IN JELLIUM

In the method developed for calculating the vibrations of ions in jellium [13], the mean-square displacement $\bar{u^2}$ was obtained in calculating $\theta_{\rm D}$ [Eq. (2)]. Here we use the root-mean-square (rms) displacement $u_{\rm rms} \equiv \sqrt{\bar{u^2}}$ as a measure of ionic freedom: when it exceeds the Wigner-Seitz radius, $r_{\rm WS} = (3m_a/4\pi\rho)^{1/3}$, the ion is effectively free. The atom-in-jellium computer program [20] was modified to calculate and output the rms fractional displacement, $u_{\rm rms}/r_{\rm WS}(\rho, T)$ (Fig. 1).

An average atom would be bound for $u_{\rm rms} < r_{\rm WS}$, with ionic heat capacity $3k_{\rm B}$, and then free for $u_{\rm rms} \geqslant r_{\rm WS}$, with heat capacity $3k_{\rm B}/2$. Given an energy distribution for the atoms, the change in heat capacity can be represented more accurately as a continuous variation with temperature. An accurate distribution could be calculated from the set of available ion-thermal energy levels populated using Boltzmann factors, but the average-atom-in-jellium method gives only a rough approximation to the states and hence to the energy levels. A simpler estimate can be made using the Maxwell-Boltzmann distribution for the velocity v of free ions,

$$f(v) = \left(\frac{m_a}{2\pi k_{\rm B}T}\right)^{3/2} 4\pi v^2 e^{-m_a v^2/2k_{\rm B}T} \qquad (7)$$

[15]. The cumulative probability distribution, giving the fraction of ions whose velocity is less than v, is

$$Pr(<v) = \mathrm{erf}\left(\sqrt{\frac{m_a v^2}{4k_{\rm B}T}}\right) - \sqrt{\frac{2m_a v^2}{\pi k_{\rm B}T}}e^{-m_a v^2/2k_{\rm B}T}. \qquad (8)$$

The minimum displacement $u_{\rm rms} = r_{\rm WS}$ for an ion to become free can be equated to a cutoff value v_c in the velocity distribution. Compared with free particles, binding between ions can be thought of as adding a saturable attractive potential. Thus, in a statistical sense, we choose to interpret v_c in terms of a characteristic binding temperature T_b for an effective number N of quadratic potential modes to become saturated,

$$\frac{1}{2}m_a v_c^2 \simeq \frac{N}{2}k_{\rm B}T_b, \qquad (9)$$

where

$$\frac{T}{T_b} = \frac{\bar{u^2}}{r_{\rm WS}^2}. \qquad (10)$$

T_b can be thought of as the temperature at which $u_{\rm rms} = r_{\rm WS}$, which might naively suggest a dependence $T_b(\rho)$. However, in our analysis, its dependence is $T_b(\rho, T)$, since $u_{\rm rms}(\rho, T)$ and $\bar{u^2}$ do not in general vary linearly with T (Fig. 2). This behavior is related to the unusual but general dependence $\theta_{\rm D}(\rho, T)$ of the jellium oscillations model, discussed above.

We have not so far found an integral of the Maxwell-Boltzmann derived heat capacity to represent the free energy in closed form, but we can generalize the similar functional form used previously [9] and derived from the partition function of a particle in a harmonic potential of finite volume [21]. This relation exhibits the desired temperature dependence for the heat capacity, giving a modification to the Debye free energy (or any other free energy f_b representing bound ions) so that the heat capacity falls at high temperature,

$$f_i = f_b - k_{\rm B}T \ \ln\left[\mathrm{erf}\left(\sqrt{\frac{NT_b}{T}}\right) - \sqrt{\frac{4NT_b}{\pi T}}e^{-NT_b/T}\right]. \qquad (11)$$

This approach is similar, except that $T/T_b(\rho, T)$ is determined directly from the average-atom calculations, and the mode

number N is expected to be a constant $o(1)$ with ρ, T, and atom type. In contrast, the approach used in the previous study [9] requires QMD simulations to be performed for at least a few temperatures and over the full range of densities of interest, for each substance.

Although we have used the generalized Debye model based on jellium oscillations, the same approach could be adopted with calculations that are more accurate for condensed matter, such as quasiharmonic phonons. The advantage of the atom-in-jellium method is the ability to predict states over a wider range in density and temperature very efficiently. In principle, a θ_D that varies with temperature as well as density can be used to represent anharmonic contributions to f_i, although atom-in-jellium calculations are unlikely to predict them as well as multiatom calculations.

IV. QUANTUM MOLECULAR DYNAMICS SIMULATIONS

QMD simulations were performed to predict the variation of ionic heat capacity c_{vi} directly. Such simulations treat the motion of the ions as classical, with three kinetic modes. The total potential energy is calculated from the electron states with respect to the instantaneous configuration of the ions at the temperature of interest. The potential contribution to the c_{vi} must thus be inferred from the total c_v, by calculating and subtracting the electronic heat capacity c_{ve} [22]. Along each isochore, c_{vi} was found to fall just as c_{ve} started to rise, so the deduced variation in $c_{vi}(T)$ was sensitive to the treatment of c_{ve}. In addition, the drop in c_{vi} started to become appreciable a little above the melt locus, so its precise variation depended on discriminating the latent heat of melting, which may be spread out in temperature in a relatively small ensemble of atoms. The entropy of melting is around $0.8k_B$/atom for most materials, though some have values between 1.5 and $4k_B$/atom [23], so melting may make a significant and insidious contribution when inferring c_{vi}.

QMD simulations were performed using the electronic structure program VASP [24]. The projector augmented wave method [25] was used, with carbon ions represented with a pseudopotential subsuming the inner two electrons. Electron wave functions were represented with a plane-wave basis set cut off at 1000 eV, at the Baldereschi mean-value point in reciprocal space [26]. Density functional theory in the local density approximation [27–29] was used for the exchange-correlation energy; some states were recalculated with the Perdew-Burke-Ernzerhof functional [30] for comparison. The simulations were in the *NVT* ensemble, using the Nosé-Hoover thermostat [31], with periodic boundary conditions. For each state of density and temperature, the motion of 64 atoms was integrated for 20 000–50 000 steps of 0.05–0.5 fs. Convergence with respect to plane-wave cutoff energy was tested at 2000 K and 5 g/cm^3 with calculations up to 3000 eV, and found to be converged to $<0.06\%$ in pressure and <4 meV/atom. Overall, given the finite cell size and use of the single mean-value k point, the pressure is likely to be converged to $<2\%$ and the energy to <10 meV/atom.

Simulations were performed along isochores at 5, 10, and 15 g/cm^3, spanning a pressure range ~0.4 to 10 TPa. Higher densities would have required a different pseudopotential subsuming fewer bound electrons, increasing the computational expense and potentially introducing systematic differences. Lower densities were not computationally tractable for simulations of the size required. However, the isochore at 5 g/cm^3 is within a small fraction of the density range to the ambient density of diamond at 3.51 g/cm^3, and so the trends in the calculations should apply down to zero pressure.

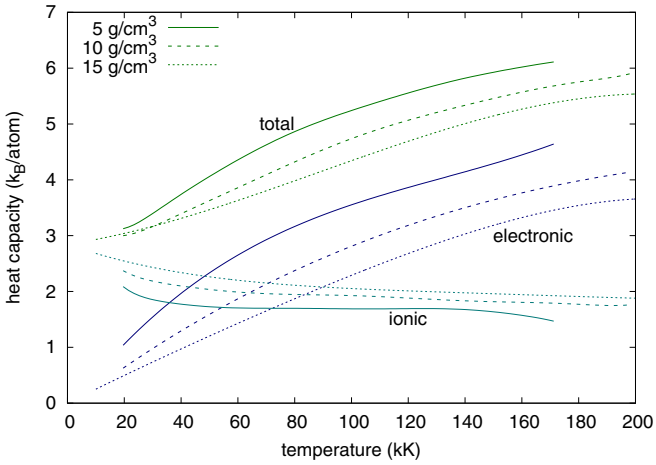

FIG. 3. Variation of heat capacities along sample isochores, deduced from QMD simulations. Fully activated vibrational modes give $3k_B$/atom, and unbound kinetic modes $\frac{3}{2}k_B$/atom.

Each simulation yielded a value for the total energy e and the electronic entropy s_e, the latter from the population of electron states. The total heat capacity was deduced from $e(T)$,

$$c_v = \left.\frac{\partial e}{\partial T}\right|_v \tag{12}$$

and the electronic heat capacity was deduced from s_e,

$$c_{ve} = T\left.\frac{\partial s_e}{\partial T}\right|_v . \tag{13}$$

In both cases, polynomials were fitted to sections of each isotherm to obtain continuous functions for which the derivatives could be evaluated. The ionic heat capoacity was then deduced as the difference,

$$c_{vi} = c_v - c_{ve}. \tag{14}$$

Given the numerical uncertainties in convergence, differentiation, and subtraction, the uncertainty in ionic heat capacity was around $0.25k_B$/atom (Fig. 3).

To interpret the QMD results, the temperature along each isochore was expressed as $\bar{u^2}/r_{WS}^2(\rho, T) \equiv T/T_b$ from the atom-in-jellium calculations. The best fit of the hypothesized free-energy function, Eq. (11), was found for $N = 0.2 \pm 0.03$ (Figs. 4 and 5). The nominal best value varied slightly using the alternative prescriptions for θ_D [Eqs. (1) and (2)] but the difference was much less than the uncertainty and the shape of $c_{vi}(T)$ was the same. The QMD results and the fit diverged systematically at low temperatures, along all three isochores. Although the deviation was within the estimated uncertainty of the QMD heat capacity, it may reflect inaccuracy of the free-energy function, Eq. (11), or of the underlying atom-in-jellium calculation.

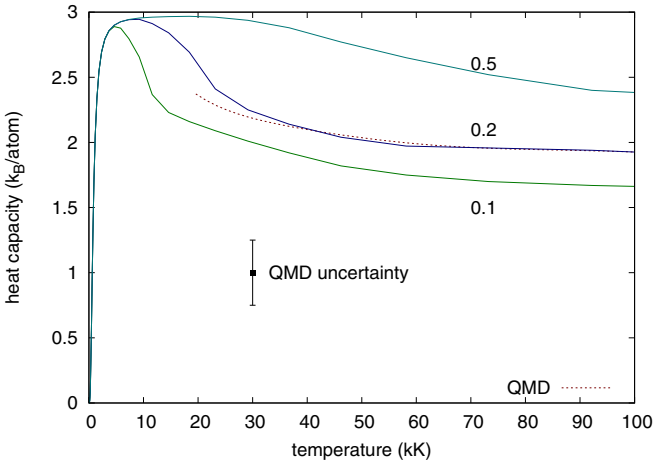

FIG. 4. Variation of ion-thermal heat capacity along the 10 g/cm^3 isochore, from QMD (dashed) and atom-in-jellium with different values of the parameter N in Eq. (11) (solid).

The atom-in-jellium method is usually inaccurate around ambient conditions as the method ignores molecular bonding and angular forces between atoms, particularly where they stabilize structures far from close-packed. The approach described here for estimating ion-thermal effects in the fluid and plasma is unlikely to be adequate when the underlying atom-in-jellium is inaccurate. However, we have found that atom-in-jellium EOS are often accurate at low temperatures (even in the solid) and high pressures. Even if the atom-in-jellium EOS fails to capture the precise details of the ionic heat capacity as it starts to fall as the fluid is heated, it is probably adequate in situations where the system passes through these conditions as is usual in high-energy-density experiments and applications.

V. EQUATION OF STATE FOR CARBON

Several wide-range EOS models have been constructed for C, mostly using Thomas-Fermi theory for high compressions and temperatures. We compare against one such EOS

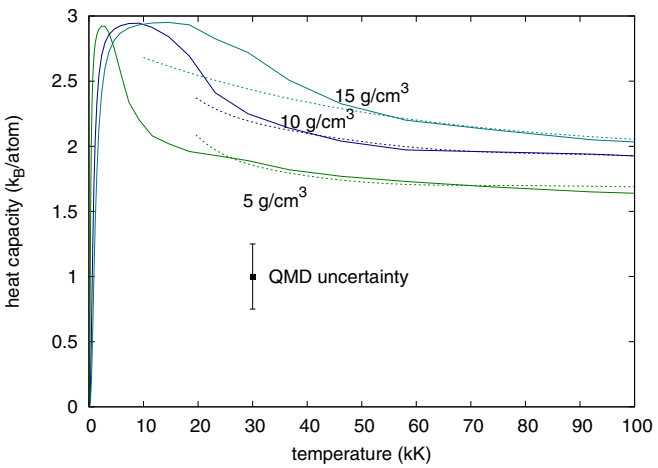

FIG. 5. Variation of ion-thermal heat capacity along sample isochores, from QMD (dashed) and atom-in-jellium with $N = 0.2$ (solid).

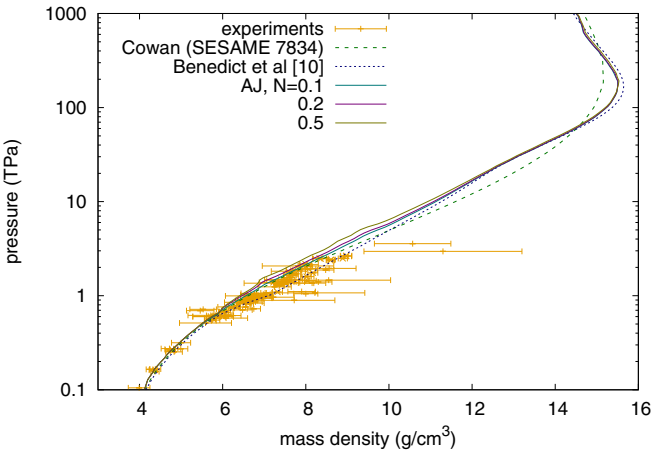

FIG. 6. Principal shock Hugoniot for carbon calculated using previous EOS models [9,32], atom-in-jellium (AJ) predictions using different values of the parameter N in Eq. (11), and compared with experimental data [35]. Where distinguishable, the solid curves are $N = 0.1$ (lower), 0.2 (middle), and 0.5 (upper).

employing a Cowan-like ion-thermal model, SESAME EOS 7834 [32], which was constrained by QMD calculations and Hugoniot measurements up to shock melting, but does not include the melting transition explicitly. In contrast, the five-phase EOS model [9] used atom-in-jellium calculations for the electron-thermal contribution only, and was constructed to include an explicit melting transition. In our present approach, the electronic component and Debye ionic component were constructed using the procedure described previously [14], and the ionic component was modified as above [Eq. (11)] to account statistically for freedom at high ion velocities. We used the displacement calculation of Debye temperature [Eq. (2)] for consistency with the use of the rms displacement in the high-temperature ionic heat capacity. The energy cal-

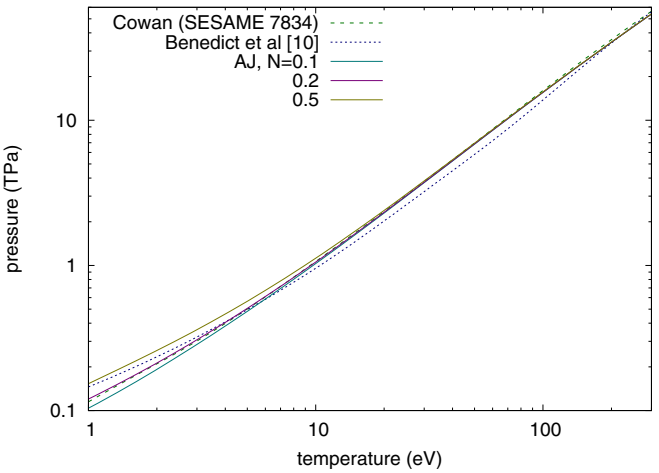

FIG. 7. Ambient isochore (3.51 g/cm^3) for carbon from previous EOS models [9,32], compared with atom-in-jellium (AJ) predictions using different values of the parameter N in Eq. (11). Where distinguishable, the solid curves are $N = 0.1$ (lower), 0.2 (middle), and 0.5 (upper).

culation [Eq. (1)] would not be significantly different on the scales considered here.

The principal shock Hugoniot was deduced by numerical solution [33,34] for each EOS model. The treatment of ionic freedom caused a variation of up to 20% in pressure between 6 and 12 g/cm^3 (1 and 10 TPa), large enough to investigate experimentally (Figs. 6 and 7).

VI. CONCLUSIONS

Atom-in-jellium estimates of thermal vibrations of the ion were used to construct a model of the reduction in ionic heat capacity at high temperatures as the ions become free. The model has a single free parameter, equivalent to the effective number of potential modes that must be saturated before the high-energy tail of the Maxwell-Boltzmann distribution describes free particles. This parameter was investigated using molecular dynamics simulations and found to be 0.2 ± 0.03, with a weak dependence on compression.

Carbon was chosen as a prototype material as its atomic number is low, emphasizing changes in the ionic heat capacity compared with the electrons, and it is widely used as a sample and ablator in high-pressure experiments. The principal shock Hugoniot and ambient isochore showed a modest sensitivity to the treatment of ionic heat capacity, which may be experimentally detectable.

Atom-in-jellium predictions of electronic states in warm dense matter were previously shown to reproduce the more rigorous approaches of PIMC and QMD. The work reported here extends the atom-in-jellium based treatment of ion-thermal energies into the dense plasma regime, and means it is now possible to calculate all contributions to the EOS self-consistently, and efficiently enough to construct an entire wide-range EOS model for an element in a few CPU hours at most. In particular, atom-in-jellium calculations can readily be performed in regimes where PIMC and QMD themselves are intractable.

ACKNOWLEDGMENTS

The QMD calculations were performed at the LLNL High-Performance Computing Facility. This work was performed under the auspices of the US Department of Energy under Contract No. DE-AC52-07NA27344.

[1] Prominent examples are the Los Alamos and Lawrence Livermore National Laboratories' EOS libraries: S. P. Lyon and J. D. Johnson, Los Alamos National Laboratory Report No. LA-UR-92-3407 (1992); D. A. Young and E. M. Corey, J. Appl. Phys. **78**, 3748 (1995).
[2] R. Grover, J. Chem. Phys. **55**, 3435 (1971).
[3] C. W. Cranfill and R. More, Los Alamos Scientific Laboratory Report No. LA-7313-MS (1978); R. M. More, K. H. Warren, D. A. Young, and G. B. Zimmerman, Phys. Fluids **31**, 3059 (1988).
[4] J. D. Johnson, High Press. Res. **6**, 277 (1991).
[5] A. L. Kritcher, T. Döppner, C. Fortmann, T. Ma, O. L. Landen, R. Wallace, and S. H. Glenzer, Phys. Rev. Lett. **107**, 015002 (2011).
[6] A. M. Saunders, A. Jenei, T. Döppner, and R. W. Falcone, Rev. Sci. Instrum. **87**, 11E724 (2016).
[7] E. L. Pollock and D. M. Ceperley, Phys. Rev. B **30**, 2555 (1984).
[8] For example, L. Collins, I. Kwon, J. Kress, N. Troullier, and D. Lynch, Phys. Rev. E **52**, 6202 (1995).
[9] L. X. Benedict, K. P. Driver, S. Hamel, B. Militzer, T. Qi, A. A. Correa, A. Saul, and E. Schwegler, Phys. Rev. B **89**, 224109 (2014); Note: in Eq. (11) of this reference, the exponent is positive, which gives a heat capacity of $2.5k_B$ as $T \to 0$. The negative exponent gives $3k_B$, as desired.
[10] K. P. Driver and B. Militzer, Phys. Rev. E **95**, 043205 (2017).
[11] D. A. Liberman, Phys. Rev. B **20**, 4981 (1979).
[12] L. H. Thomas, Proc. Cambridge Philos. Soc. **23**, 542 (1927); E. Fermi, Rend. Accad. Naz. Lincei. **6**, 602 (1927).
[13] D. A. Liberman and B. I. Bennett, Phys. Rev. B **42**, 2475 (1990).
[14] D. C. Swift, T. Lockard, R. G. Kraus, L. X. Benedict, P. A. Sterne, M. Bethkenhagen, S. Hamel, and B. I. Bennett, Phys. Rev. E **99**, 063210 (2019).
[15] J. R. Waldram, *The Theory of Thermodynamics* (Cambridge University Press, Cambridge, UK, 1985).
[16] For example, D. J. Steinberg, Lawrence Livermore National Laboratory Report No. UCRL-MA-106439 change 1 (1996).
[17] P. Debye, Ann. Phys. **344**, 789 (1912).
[18] D. C. Swift, G. J. Ackland, A. Hauer, and G. A. Kyrala, Phys. Rev. B **64**, 214107 (2001).
[19] A. A. Correa, L. X. Benedict, D. A. Young, E. Schwegler, and S. A. Bonev, Phys. Rev. B **78**, 024101 (2008).
[20] B. I. Bennett and D. A. Liberman, Los Alamos National Laboratory Report No. LA-10309-M (1985).
[21] A. A. Correa, L. X. Benedict, M. A. Morales, P. A. Sterne, J. I. Castor, and E. Schwegler, arXiv:1806.01346.
[22] H. D. Whitley, D. M. Sanchez, S. Hamel, A. A. Correa, and L. X. Benedict, Contrib. Plasma Phys. **55**, 390 (2015).
[23] E. Chisolm, Los Alamos National Laboratory Report No. LA-UR-10-08329 (2010).
[24] G. Kresse and J. Furthmüller, Phys. Rev. B **54**, 11169 (1996).
[25] P. E. Blöchl, Phys. Rev. B **50**, 17953 (1994).
[26] A. Baldereschi, Phys. Rev. B **7**, 5212 (1972).
[27] P. Hohenberg and W. Kohn, Phys. Rev. **136**, B864 (1964).
[28] W. Kohn and L. J. Sham, Phys. Rev. **140**, A1133 (1965).
[29] J. P. Perdew, J. A. Chevary, S. H. Vosko, K. A. Jackson, M. R. Pederson, D. J. Singh, and C. Fiolhais, Phys. Rev. B **46**, 6671 (1992).
[30] J. P. Perdew, K. Burke, and M. Ernzerhof, Phys. Rev. Lett. **77**, 3865 (1996).
[31] W. G. Hoover and B. L. Holian, Phys. Lett. A **211**, 253 (1996).
[32] S. Crockett, documentation for SESAME EOS 7834, Los Alamos National Laboratory (2006).
[33] D. C. Swift, J. Appl. Phys. **104**, 073536 (2008).
[34] D. C. Swift and M. Millot (unpublished).
[35] M. N. Pavlovskii, Sov. Phys. Solid State **13**, 741 (1971); K. Kondo and T. J. Ahrens, Geophys. Res. Lett. **10**, 281 (1983); D. Bradley, J. H. Eggert, D. G. Hicks, P. M. Celliers, S. J. Moon,

R. C. Cauble, and G. W. Collins, Phys. Rev. Lett. **93**, 195506 (2004); H. Nagao, K. G. Nakamura, K. Kondo, N. Ozaki, K. Takamatsu, T. Ono, T. Shiota, D. Ichinose, K. A. Tanaka, K. Wakabayashi, K. Okada, M. Yoshida, M. Nakai, K. Nagai, K. Shigemori, T. Sakaiya, and K. Otani, Phys. Plasmas **13**, 052705 (2006); S. Brygoo, E. Henry, P. Loubeyre, J. Eggert, M. Koenig, B. Loupias, A. Benuzzi-Mounaix, and M. R. Le Gloahec, Nat. Mater. **6**, 274 (2007); D. G. Hicks, T. R. Boehly, P. M. Celliers, D. K. Bradley, J. H. Eggert, R. S. McWilliams, R. Jeanloz, and G. W. Collins, Phys. Rev. B **78**, 174102 (2008); R. S. McWilliams, J. H. Eggert, D. G. Hicks, D. K. Bradley, P. M. Celliers, D. K. Spaulding, T. R. Boehly, G. W. Collins, and R. Jeanloz, *ibid.* **81**, 014111 (2010); M. D. Knudson, M. P. Desjarlais, and D. H. Dolan, Science **322**, 1822 (2008); M. C. Gregor, D. E. Fratanduono, C. A. McCoy, D. N. Polsin, A. Sorce, J. R. Rygg, G. W. Collins, T. Braun, P. M. Celliers, J. H. Eggert, D. D. Meyerhofer, and T. R. Boehly, Phys. Rev. B **95**, 144114 (2017).